

# Single-beat Measurement of Left Ventricular Contractility in Normothermic *Ex Situ* Perfused Porcine Hearts

Weiping Xiao, Liming Xin\*, Shouwei Gao, Yan Peng, Jun Luo, Weiran Yao, Roberto Ribeiro, Zhibing Xu, Zhenyu Zhang, Yuanyuan Liu, Jianhui Li, Mitesh Badiwala, and Yu Sun

**Abstract— Objective:** For heart transplantation, donor heart status needs to be evaluated during normothermic *ex situ* perfusion (ESHP). Left ventricular end-systolic elastance ( $E_{es}$ ) measures the left ventricular contractile function, but its estimation requires the occlusion of the left atrium line in the ESHP, which may cause unnecessary damage to the donor heart. We present a novel method to quantify  $E_{es}$  based on hemodynamic parameters obtained from only one steady-state PV loop in ESHP. **Methods:**  $E_{es}$  was obtained by the end-systolic point ( $P_{es}$ ,  $V_{es}$ ) and the volume axis intercept point of  $E_{es}$  ( $V_0$ ).  $V_0$  was estimated through the support vector machine regression (SVR) method using parameters derived from the measured steady-state PV loop. To achieve high  $V_0$  estimation accuracy, a filter-based support vector machine recursive feature elimination method (SVM-RFE) algorithm selected the parameters for  $V_0$  estimation. Hemodynamic parameter samples ( $n = 101$ ) obtained from ESHP experiments with pig's hearts were used to train the  $E_{es}$  calculation model. Early post-transplantation outcomes in six heart transplantation experiments were then estimated from the trained  $E_{es}$  calculation model. **Results:**  $E_{es}$  calculated by the proposed method agreed well with conventional multi-beat estimates obtained by the occlusion process ( $r = 0.88$ ,  $p < 0.001$ ,  $n = 101$ ) and was capable of predicting the early post-transplant cardiac index ( $r = 0.84$ ,  $p < 0.05$ ,  $n = 6$ ). **Conclusion:** This method effectively assesses left ventricular contractility during ESHP and predicts early post-transplant outcomes in the porcine model. **Significance:** Our approach is the first to quantify  $E_{es}$  by estimating  $V_0$  from steady-state beats in ESHP for accurately predicting early post-transplantation outcomes.

**Index Terms—***Ex situ* heart perfusion, left ventricular contractility, machine learning, heart transplantation.

There is no conflict of interest. Asterisk indicates corresponding author.

W. Xiao, S. Gao, Y. Peng, Z. Xu, Z. Zhang and Y. Liu are with the School of Mechatronic Engineering and Automation, Shanghai University, Shanghai, China.

L. Xin\* is with Shanghai University, China and also with the Department of Mechanical & Industrial Engineering, University of Toronto, Toronto, ON, Canada (correspondence email: xin\_liming@hotmail.com).

J. Luo is with the State Key Laboratory of Mechanical Transmissions, Chongqing University, Chongqing, China.

W. Yao is with the School of Astronautics, Harbin Institute of Technology, Harbin, China.

R. Ribeiro and M. Badiwala are with the Faculty of Medicine, University of Toronto, Toronto, ON, Canada.

J. Li is with the Division of Hepatobiliary and Pancreatic Surgery, Department of Surgery, Key Lab of Combined Multi-Organ Transplantation, Ministry of Public Health, First Affiliated Hospital, Zhejiang University School of Medicine, Hangzhou, China.

Y. Sun is with the Department of Mechanical & Industrial Engineering, University of Toronto, Toronto, ON, Canada.

Copyright (c) 2017 IEEE. Personal use of this material is permitted. However, permission to use this material for any other purposes must be obtained from the IEEE by sending an email to pubs-permissions@ieee.org.

## I. INTRODUCTION

HEART transplantation is the gold-standard treatment for eligible patients with end-stage heart failure [1], [2]. Organ shortage is a challenge in heart transplantation. The low utilization rate of donor hearts contributes to this organ shortage. Only ~35% of donor-brain death (DBD) hearts are used for transplantation [3]. Most of the myocardium in such discarded hearts is histologically normal and observed organ dysfunction may be reversible [4]. Moreover, marginal organs and organs from donation after circulatory death (DCD) may be an additional source of organs for transplantation. Cold static storage (CS) is a simple and inexpensive standard organ preservation method. However, CS fails to provide a portal for assessment of graft viability (e.g., myocardial function, metabolic function, etc.) prior to transplantation, placing the recipient at risk of transplantation failure [5]. Moreover, CS might bring myocardial injury in the low-temperature environment [6]. A quantitative method to evaluate the donor hearts viability prior to transplantation is required before discarded hearts from DBD and DCD donors can be utilized clinically. Normothermic *ex situ* heart perfusion (ESHP) maintains donor hearts normal metabolism in beating state, providing the opportunity to assess organ viability prior to transplantation [7]–[10]. The slope of end-systolic pressure-volume relationship (ESPVR) is a useful measure of the left ventricular (LV) contractile function, and  $E_{es}$  has been shown to be a load-insensitive index of ventricular contractility [11]. This makes  $E_{es}$  a reliable and effective parameter to evaluate donor heart function in ESHP.

Conventionally,  $E_{es}$  is measured by changing the left ventricular preload or afterload conditions, such as through inferior vena cava occlusion (decrease blood input), and simultaneously acquiring multiple pressure-volume (PV) loops to build the ESPVR [12], [13]. However, for ESHP, the traditional measurement methods have three problems. First, decreasing the heart blood input causes damages to the donor heart, such as tissue hypoxia, ischemic injury, and arrhythmia [14]–[16]. Second, traditional measurement methods cannot achieve real-time measurements and treat heart problems in time. Finally, it is difficult to generate multiple steady-state PV loops in the ESHP setting, because isolated hearts are usually loaded at a relatively low volume compared to *in vivo* hearts for recovery. Lower LV volume usually generates low-accuracy PV loops, especially during the occlusion process, making the extraction

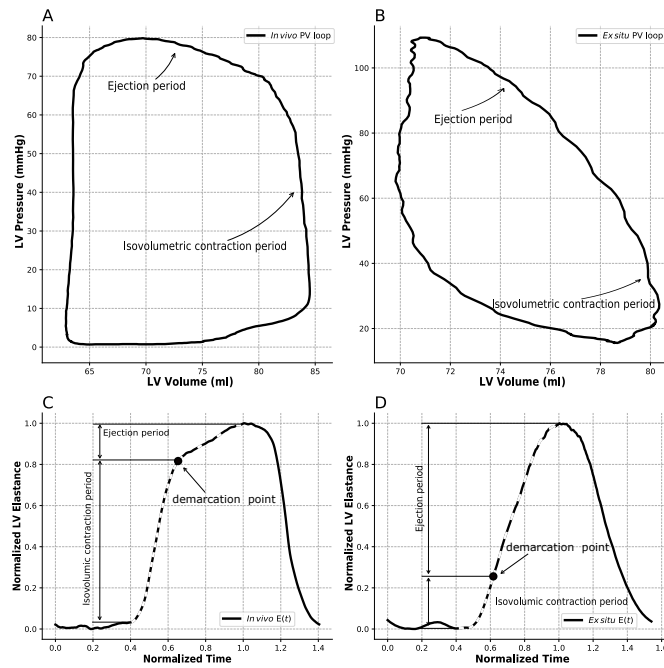


Fig. 1. A. Representative *in vivo* PV loop. B. Representative *ex situ* PV loop. C. *In vivo* normalized time-varying  $E(t)$ . D. *Ex situ* normalized time-varying  $E(t)$ . Compared with the *in vivo* PV loop, there is no clear isovolumetric contraction phase in the PV loop of the *ex situ* perfused heart. Left ventricular elastance is normalized here. Compared with *in vivo*  $E(t)$ , there is no clear demarcation point between the isovolumetric contraction and the ejection phase of the curve, and the two curves cannot be estimated using a bilinear function.

of  $E_{es}$  through these loops difficult.

Several *in vivo*  $E_{es}$  estimation methods have been reported. The theoretically existing peak isovolumetric pressure  $P_{max}$  was introduced to calculate  $E_{es}$  [17]–[20]. Attempts were also made to estimate  $E_{es}$  using geometric features of time-varying elastic curves  $E(t)$  [21], [22]. However, these  $E_{es}$  estimates all depend on the stable *in vivo* PV loops with clear isovolumetric contraction and ejection phases (Fig. 1A and C), which are difficult to obtain in ESHP because isovolumetric systole and ejection phases measured *in vitro* are difficult to identify (Fig. 1B and D). Therefore, existing  $E_{es}$  evaluation methods cannot be directly applied to ESHP experiments. A less invasive (no occlusion process) and more reliable  $E_{es}$  calculation method is needed to replace the traditional occlusion method in ESHP.

In this work, we developed a method to calculate  $E_{es}$  by predicting  $V_0$  (LV unstressed volume) in normothermic ESHP. The problems tackled in this work include: (1) How to calculate  $E_{es}$  on the deformed PV loop through a single heart beat; (2) How to select stable and reliable key features from the numerous hemodynamic parameters obtained in ESHP experiments; and (3) How to construct a  $V_0$  prediction model with high precision and good generalization ability (i.e., the ability to predict  $V_0$  of a heart outside of the training set).

To solve these challenges, the main contributions of this paper are as follows: (1) A  $V_0$ -based  $E_{es}$  calculation method for ESHP is proposed that does not require an occlusion operation and is applied for deformed PV loops. (2) An improved support vector machine recursive feature elimination method



Fig. 2. PV loop measurement in *ex situ* heart perfusion system.

(SVM-RFE) [23], [24] is proposed to screen the low accuracy and redundant features by introducing the intraclass correlation coefficient (ICC) [25] and correlation coefficient analysis. (3) An support vector machine regression (SVR) [26]–[28] model is proposed to predict  $V_0$  from the selected key hemodynamic parameters accurately. ESHP experiments are performed to evaluate the proposed  $E_{es}$  calculation method. Experimental results show that the method is able to accurately predict  $V_0$  and  $E_{es}$  with the prediction accuracy of 0.99 and 0.88, respectively. We also performed animal (pig) experiments, and the results show that  $E_{es}$  calculated during ESHP was in good correlation with the cardiac index (CI) after transplantation ( $r = 0.84$ ,  $p < 0.05$ ,  $n = 6$ ). To our best knowledge, this is the only study to date that quantifies  $E_{es}$  by estimating  $V_0$  from steady-state beats in ESHP, which enables accurate prediction of early post-transplantation outcomes (CI).

## II. MATERIALS AND METHODS

### A. Animal Experiments

Our institutional animal care committee approved all experimental protocols, and animals were treated following the Guide for the Care and Use of Laboratory Animals prepared by the Institute of Laboratory Animal Resources, National Research Council, 1996.

#### 1) Experimental preparation:

Thirty-three male Yorkshire pigs ( $55 \pm 5$  kg) were used in this study, 27 of which for *ex situ* perfusion experiments and 6 for transplantation experiments. Animals were pre-medicated with an intramuscular injection of midazolam (0.3 mg/kg) and ketamine (20 mg/kg). Anesthetic maintenance was done using a 1%–2% inspiratory fraction of isoflurane through an oral endotracheal tube. After median sternotomy and dissection of the cardiac structures, 30,000 units of heparin were given intravenously. A conductance catheter (SPC-571, Millar Inc., Houston, TX) was inserted transapically into the left ventricle for contractility assessment using pressure-volume loops. Following the baseline cardiac evaluation, 1.5 L of blood was collected from the inferior vena cava, and

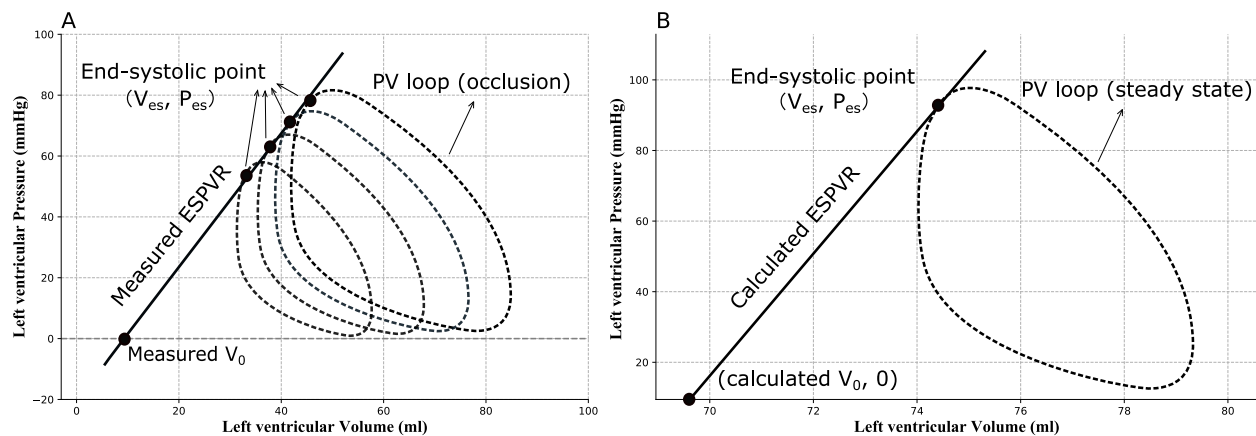


Fig. 3. A. Schematic diagram of the traditional  $E_{es}$  measurement method. B. Schematic diagram of the proposed  $E_{es}$  calculation method. The solid line represents ESPVR, and its slope is  $E_{es}$ . The dashed line is the measured PV loop. The traditional method requires occlusion of the vena cava to obtain multiple PV loops measured under different load conditions and then regression analysis of the coordinates of the end-systolic on each PV loop to obtain  $E_{es}$ . The single-beat method requires only a single PV loop measured at steady-state and  $V_0$  calculated from the PV loop to obtain  $E_{es}$ .

the heart was arrested with 1,000 mL of cardioplegic solution at 4°C. The heart was excised and placed in the ice-cold cardioplegic solution for 1 h. The aorta, pulmonary artery, superior vena cava, and left atrium were cannulated, and the inferior vena cava was ligated for ESHP during this period. The ESHP system was primed with 1.5 L of autologous blood along with 1 g of Cefazolin, 2 g of magnesium sulfate, and 10,000 units of heparin. A hematocrit of 20% was achieved by adding STEEN Solution™ (EX VIVO Perfusion, Goteborg, Sweden). The partial pressure of O<sub>2</sub> and CO<sub>2</sub> was maintained between 100 and 300 mmHg and between 35 and 45 mmHg, respectively. Dobutamine (5 mcg/min) and Insulin (5 units/h) were infused continuously throughout the experiment (Fig. 2).

### 2) Ex situ perfusion experiment:

After 1 h of cold storage, the reperfusion of the heart was started on the customized ESHP system [29]. Retrograde aortic flow with the constant pressure of 50 mmHg was maintained for 4 h. Left and right atrial pressures were kept at 0 mmHg. All hearts ( $n = 27$ ) were transitioned from Langendorff mode to working mode at 1, 4, and 5 h for functional assessment. A conductance catheter (SPC-571, Millar Inc., Houston, TX) was inserted through the ascending aorta to the left ventricle for the PV. Each measurement was repeated three times.

### 3) Transplantation experiment:

Six hearts were procured and perfused *ex situ* for 4 h (3 h of Langendorff perfusion and then 1 h of bi-ventricular working mode for functional assessment). Left ventricular function was assessed as described in *ex situ* perfusion experiment in working mode. After 4 h perfusion, the heart was flushed with the cardioplegic solution. The recipient pigs were prepared as described in experimental preparation. The heart-lung machine was prepared and connected to the recipient pig after mid-line sternotomy and pericardial dissection. The donor's heart was implanted after removing the recipient pig heart. After weaning, the cardiac output was measured using an invasive Swans-Ganz catheter 3 h after post-transplant reperfusion [30].

### B. E<sub>es</sub> Quantification

We propose a new method to calculate  $E_{es}$  by predicting  $V_0$ , which does not require multiple occlusions of the left atrium line and minimizes damage to the heart. The single-beat  $E_{es}$  calculation approach is based on the premise that ESPVR is linear in the measured range [19], and  $V_0$  is treated as a constant under different loading conditions if the interest is confined to  $E_{es}$  [20], [31].  $V_0$  is the ventricular volume at zero pressure (often referred to as “unstressed volume”).  $E_{es}$  is given by [22]:

$$E_{es} = \frac{P_{es}}{V_{es} - V_0}, \quad (1)$$

where  $P_{es}$  and  $V_{es}$  are the end-systolic pressure and volume in the steady-state PV loop, respectively (Fig. 3B). Based on Eq. 1,  $E_{es}$  could be obtained from any steady-state beat once  $V_0$  is known. However, the traditional calculation method of  $V_0$  can only be calculated by multiple PV loops [32]. Previous studies show that  $V_0$  has a strong correlation with measurable heart functional parameters in steady-state beat PV loop (e.g., end-systolic volume, pressure-volume area, and heart rate) [21], [32]–[34]. SVR has been proven to be an effective tool for solving the regression problem with a small sample size [35]–[37]. Here, we introduce the SVR method to estimate  $V_0$  using hemodynamic parameters (features) obtained from the steady-state PV loop. An SVM-RFE algorithm is proposed to select the key features used in the SVR model.

The proposed  $E_{es}$  calculation has the following four steps (Fig. 4).

#### 1) Data acquisition and preprocessing:

One hundred and forty-four steady-state PV loop measurement samples from 27 ESHP experiments were recorded. Thirty-four hemodynamic parameters (e.g., end-systolic pressure, cardiac output, ejection fraction, etc.) were derived from each steady-state PV loop using the IOX software (emka TECHNOLOGIES S.A., 75015 Paris, France), serving as a feature set for machine learning. All the 144 PV loop measurement samples were randomly divided into two groups

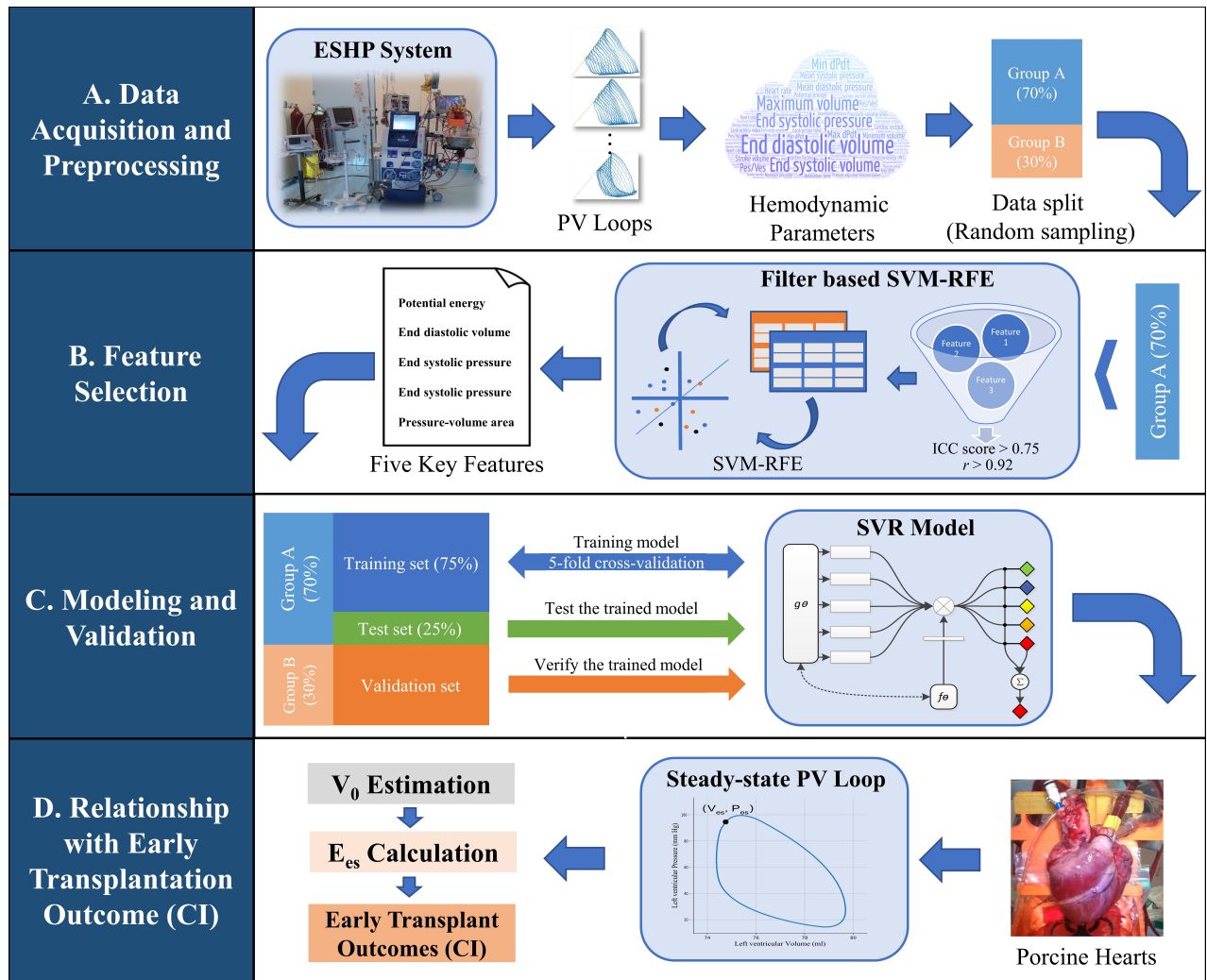


Fig. 4.  $E_{es}$  calculation involves four steps. Step 1 data acquisition and preprocessing: steady-state PV loop measurement samples were recorded and hemodynamic parameters were derived from each steady-state PV loop, these samples were randomly divided into two groups by standard randomization; Step 2 feature selection: low reliable features were screened by ICC score, and then the rest of the features were classified by correlation analysis, one representative feature in each class is kept for the next step, at last, key features are selected using SVM-RFE from the representative features; Step3 modeling and validation: Group A were split into a training set and a testing set randomly, a fivefold cross-validation was performed in the training process to obtain the optimal parameters of SVR, and SVR performance was assessed in the testing set. The trained SVR model was verified in group B. Step 4: heart transplantation experiments were performed to study the correlation between  $E_{es}$  and early post-transplant cardiac.

by standard randomization (“train\_test\_split” function in the Scikit-learn library [38]). Group A contains 101 samples (70%), which were used to build and test the SVR model, and group B contains the remaining 43 samples (30%), which were used to validate the model. Each measurement sample contains at least three repeated PV loop measurements.

### 2) Filter-based feature selection:

$V_0$  is estimated using the SVR method based on the features (34 hemodynamic parameters aforementioned) obtained from the steady-state PV loop. In order to reduce the complexity of the algorithm and achieve high estimation accuracy, we propose a filter-based SVM-RFE algorithm to select key features (hemodynamic parameters) for the SVR model (Fig. 4B). All the samples in group A were used in this feature selection process. There are three steps in this feature selection process.

First, ICC score is introduced to screen the features with

low reliability. Compared to the *in vivo* measurement, ESHP partially loads the heart, which reduces the reliability of some parameters derived from the measured PV loop. In the proposed algorithm, the reliability of each parameter is verified and selected by ICC using a single-measurement, absolute-agreement, two-way mixed-effects model (feature with an ICC score greater than 0.75 is considered as a reliable feature [39]). Features with high reliability are selected by

$$A = \{c | I(c) > k_1, c \in X\}, \quad (2)$$

where  $A$  is a feature subset screened by the index ICC,  $c$  is the candidate feature,  $X$  is the candidate feature set,  $I(c)$  is the intraclass correlation coefficient of feature  $c$ , and  $k_1$  is set to be 0.75.

Then, features are classified through correlation coefficient analysis [40], In each class, one representative feature is

selected for the next step and the rest of the features are screened according to

$$B = \{c_i | R(c_i, c_j) < k_2, c_j \in A, c_i \in A, c_j \neq c_i\}, \quad (3)$$

where  $B$  is the representative feature subset,  $c_i$  represents a candidate feature,  $c_j$  represents the feature in  $A$  that is different from  $c_i$ , and  $R(c_i, c_j)$  represents a correlation coefficient between  $c_i$  and  $c_j$ ; here,  $k_2 = 0.92$ .

Lastly, the key features (subset  $C$ ) are selected using SVM-RFE from the representative features (subset  $B$ ). This process traverses all the possible combinations of features in the feature subset  $B$  using a sequential backward selection method, and the selection criterion is

$$\text{Estimation accuracy} = \left(1 - \frac{V_{\text{calculated}} - V_{\text{measured}}}{V_{\text{measured}}}\right) * 100\%, \quad (4)$$

where  $V_{\text{calculated}}$  represents the calculated value of  $V_0$ , and  $V_{\text{measured}}$  represents  $V_0$  derived from the measured PV loop. The key feature (subset  $C$ ) with the highest prediction accuracy is selected.

### 3) Modeling and validation:

Group A were split into a training set (75%) and a testing set (25%) randomly using standard randomized “train\_test\_split” in the Scikit-learn library (Fig. 4A). A five-fold cross-validation was performed in the training process to obtain the optimal parameters of SVR, and SVR performance was assessed in the testing set. The trained SVR model based on the features selected by the SVM-RFE and filter-based SVM-RFE algorithm was verified in group B.

$V_0$  and  $E_{\text{es}}$  obtained from the SVR model were compared with  $V_0$  and  $E_{\text{es}}$  derived from the conventional method, respectively (Fig. 3). The coefficient of determination ( $R^2$ ) was introduced as the criteria to evaluate model performance. Bland-Altman plot was also introduced to compare the proposed  $E_{\text{es}}$  measurement with the conventional method.

### 4) Relationship with early transplantation outcomes (CI):

In transplantation experiments, six donor pig hearts were perfused *ex situ* for 4 h and then transitioned into the working mode for function assessment.  $E_{\text{es}}$  was calculated by the proposed method. Linear regression was performed to study the correlation between  $E_{\text{es}}$  and early post-transplant cardiac index.

## C. Statistical Analysis

All data are expressed as mean standard deviation (SD), and a  $p$ -value  $< 0.05$  is considered statistically significant. For the variables which are normally distributed, we use Pearson correlation; for those that do not follow normal distribution, we use Spearman correlation. A comparison of steady-state beat and multi-beat estimates of  $V_0$  and  $E_{\text{es}}$  was performed by linear regression analysis. Statistical analysis was performed with commercial software (SPSS 22.0; SPSS, Chicago, IL, USA).

## III. RESULTS AND DISCUSSION

We developed and validated a novel approach for  $E_{\text{es}}$  calculation in ESHP. Compared with the traditional method,

TABLE I  
RESULT OF FEATURE SELECTION

Indicators	SVM-RFE Algorithm	Filter-based SVM-RFE Algorithm
Feature subset	EF, $V_{\text{ed}}$ , $P_{\text{es}}/V_{\text{es}}$ , $V_{\text{max}}$ , $V_{\text{min}}$ , PE, PE-MEC, PVA, SW	$V_{\text{ed}}$ , $P_{\text{es}}$ , $V_{\text{es}}$ , PE-MEC, PVA
Feature dimension	9	5
Feature reliability	$0.69 \pm 0.28$	$0.83 \pm 0.06$
Solution space for feature selection	$2^{34}$	$2^{20}$
$V_0$ estimation accuracy (test set in group A)	$0.93 \pm 0.06$	$0.95 \pm 0.04$
$V_0$ estimation accuracy (group B)	$0.64 \pm 0.72$	$0.90 \pm 0.12$
Paired t test (SVM-RFE vs Filter based SVM-RFE)	$p = 0.153$ (group A)	$p = 0.014$ (group B)

EF = ejection fraction,  $P_{\text{es}}/V_{\text{es}}$  = end-systolic pressure / end-systolic volume,  $V_{\text{max}}$  = maximum volume,  $V_{\text{min}}$  = minimum volume, PE = potential energy, and SW = stroke work. The number of solution space states of the  $N$  features is  $2^N$ . A paired t test was used to test whether the prediction accuracy based on SVM-RFE and filter-based SVM-RFE methods in group A (test set) and group B was significantly different.

our method calculates  $E_{\text{es}}$  by estimating  $V_0$  from the steady-state beat PV loop in ESHP to avoid multiple occlusion and reduce the injury to the heart. To establish an accurate and reliable  $V_0$  prediction model, we propose a filter-based SVM-RFE algorithm to screen the poor reliability and redundant features. Features with lower feature dimensions and higher reliability on the premise of ensuring the estimation accuracy (Table I) are selected for the SVR model. Experimental results (Fig. 6) show that  $V_0$  and  $E_{\text{es}}$  obtained by the proposed method correlated well with the conventional method over a wide range of cardiac contractility and loading conditions. Transplantation experiments confirmed that  $E_{\text{es}}$  calculated by our experiments correlated well with the early post-transplant cardiac index (Fig. 7).

### A. Feature Selection

SVR has been widely used for regression with a number of features [26]–[28]. Creating an SVR model based on the most relevant features can achieve high accuracy and reduce model complexity. SVM-RFE has been shown to be a powerful feature selection algorithm [23], [24]. However, estimation results may be biased when there are highly correlated features. For example, in our work,  $P_{\text{max}}$  and  $P_{\text{es}}$  are highly correlated (the values of  $P_{\text{es}}$  and  $P_{\text{max}}$  are close on a PV loop [41]), and these redundant features can cause estimation errors. Some of the features derived from steady-state PV loops are not reliable (for example, the ICC score of stroke work was 0.584), which can also reduce the accuracy of estimation results. These low-reliability features are mainly due to the fact that the heart is partially loaded in ESHP, and the volume measurement is typically not stable due to the irregular shape of the left ventricle in many hearts (the volume measurement of the left ventricle is based on the assumption that the left ventricle is a

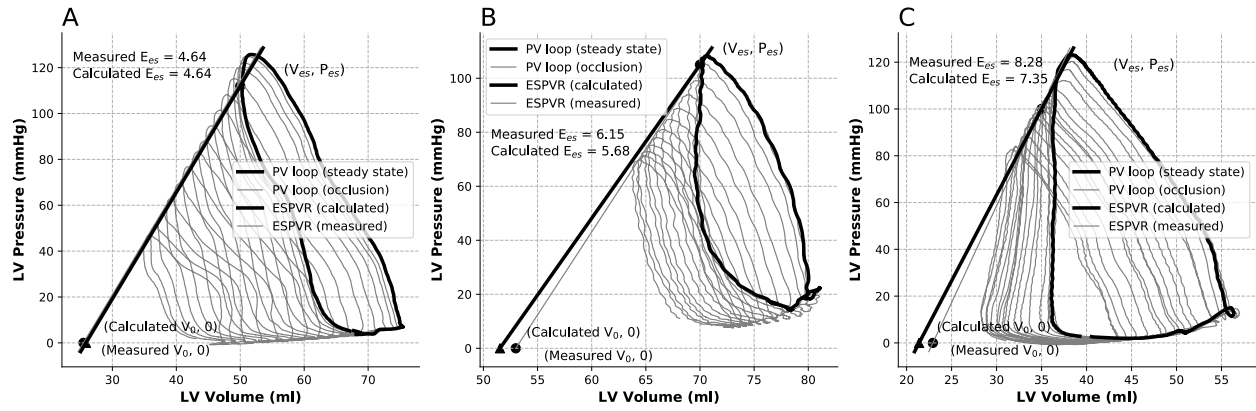


Fig. 5. Representative PV loops in *ex situ* heart perfusion experiments.  $V_0$  and  $E_{es}$  calculated by the proposed method using steady-state beat PV loop data and  $V_0$  and  $E_{es}$  derived from multi-beat PV loops are both displaced.

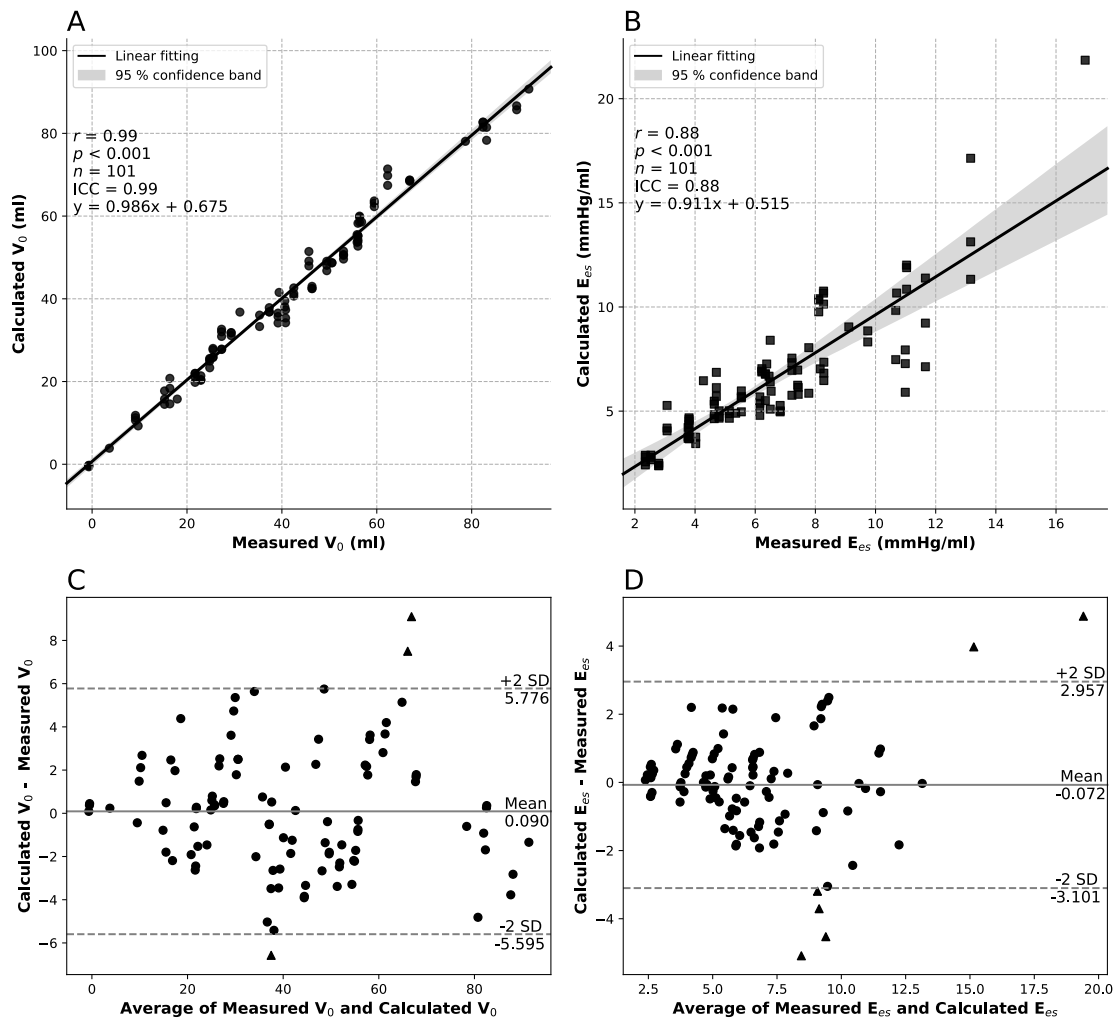


Fig. 6. A. Relationship between the calculated  $V_0$  and measured  $V_0$ . B. Relationship between the calculated  $E_{es}$  and measured  $E_{es}$ . Multi-beat data were obtained during left atrium occlusion; the single-beat calculation was made from the first steady-state beat preceding each occlusion. C. Bland-Altman analysis of calculated  $V_0$  and measured  $V_0$  values: the difference between the measured  $V_0$  and calculated  $V_0$  values is plotted against their average. D. Bland-Altman analysis of calculated  $E_{es}$  and measured  $E_{es}$  values: the difference between the measured  $E_{es}$  and calculated  $E_{es}$  values is plotted against their average.

cone). The proposed filter-based SVM-RFE algorithm has the capability of screening out low liable and redundant features.

Using the proposed feature selection algorithm, eight features with poor reliability (ICC score < 0.75) and six redun-

dant features ( $r > 0.92$ ) were excluded from the candidate feature set  $\mathbf{X}$  (34 features). After the screening, the state of feature selection solution space (complexity) was reduced from  $2^{34}$  (34 features) to  $2^{20}$  (20 features). Then five key features (end-systolic volume ( $V_{es}$ ), end diastolic volume ( $V_{ed}$ ), end-systolic pressure ( $P_{es}$ ), potential energy-MEC (PE-MEC), and pressure-volume area (PVA)) were selected by SVM-RFE from the remaining 20 features (feature subset  $\mathbf{B}$ ).

The proposed filter-based SVM-RFE algorithm and traditional SVM-RFE algorithm were compared, and the results are shown in Table . The number of key features selected using the proposed algorithm and the conventional SVM-RFE algorithm is five and nine, respectively. The features selected by the proposed algorithm have higher reliability (ICC score  $> 0.75$ ) compared to the features selected by the SVM-RFE algorithm (mean ICC score: 0.83–0.69). Features selected by the proposed algorithm and conventional algorithm from group A are put into the SVR model. The two models are trained in the training set of group A, and the trained models are verified in groups A and B (Fig. 4). The proposed algorithm has better  $V_0$  estimation accuracy in both groups, while the conventional feature selection algorithm has poor estimation accuracy in the new data set group B (group A (test set):  $0.95 \pm 0.04$  to  $0.93 \pm 0.06$  ( $p > 0.05$ ), group B:  $0.90 \pm 0.12$  to  $0.64 \pm 0.72$  ( $p < 0.05$ )). The experimental results show that the proposed method generates higher prediction accuracy and generalization performance.

### B. Validation of $V_0$ and $E_{es}$ Quantification

In our method,  $E_{es}$  is calculated by predicting  $V_0$  (Fig. 3B), which is suited for ESHP because the shape of the PV loop would have little impact on the calculation.  $V_0$  is an appropriate systolic index, and its decrease reflects the increase of left ventricular systolic function [42]. We also found that  $V_0$  has a strong correlation with many hemodynamic parameters extracted from a single PV loop. Therefore, we established a machine learning model based on hemodynamic parameters to predict  $V_0$ . In this way, invasive damage caused by the occlusion operation can be reduced as much as possible. In our study,  $E_{es}$  was successfully derived from  $V_0$ , which was obtained by the SVR algorithm through hemodynamic parameters of the steady-state PV loop.

Representative  $V_0$  and  $E_{es}$  obtained by the proposed approach and by the conventional multi-beat PV loops approach are shown in Fig. 5. Fig. 6A shows the relationship between  $V_0$  calculated by the proposed approach and  $V_0$  measured by the conventional approach ( $r = 0.99$ ,  $p < 0.001$ ,  $n = 101$ ). Fig. 6B shows the relationship of  $E_{es}$  calculated by the proposed approach and  $E_{es}$  measured by the conventional approach ( $r = 0.88$ ,  $p < 0.001$ ,  $n = 101$ ). The data indicate a strong correlation between calculated  $V_0$  and  $E_{es}$  and  $V_0$  and  $E_{es}$  obtained by the conventional multi-beat approach. We also performed Bland-Altman analysis. As shown in Fig. 6C and D, the average deviation between the calculated value and the measured value is low ( $V_0$ : 0.09 mL;  $E_{es}$ :  $-0.07$  mmHg/mL). The correlation analysis and Bland-Altman plot show that the proposed method is an acceptable way to measure  $E_{es}$ .

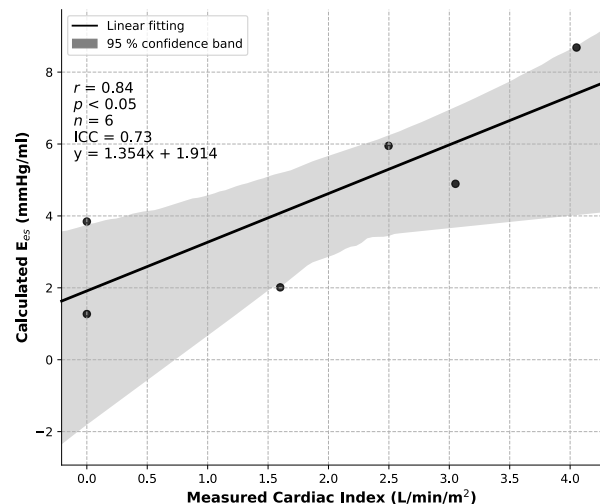


Fig. 7. Relationship between calculated  $E_{es}$  by our method and early (3 h) post-transplant cardiac index.

### C. Transplantation Results

$E_{es}$  is one of the key cardiac parameters, represents the left ventricular contractility [10], [12], [13]. Transplantation experiments were performed to investigate the relationship between the quantified  $E_{es}$  values and early post-transplant outcome (CI). The donor's heart was implanted after removing the recipient pig heart. After weaning, the cardiac output was measured using an invasive Swans-Ganz catheter 3 h after post-transplant reperfusion. As shown in Fig. 7,  $E_{es}$  obtained using the proposed approach in ESHP prior to the transplantation shows a good correlation with early post-transplant cardiac index ( $r = 0.84$ ,  $p < 0.05$ ,  $n = 6$ ). The two data with CI of 0 in Fig. 7 indicates the failure of the heartbeat. The results of the transplantation experiments show that the proposed method is a useful tool to evaluate organ viability during ESHP, which mitigates transplantation risks and effectively utilizes marginal donor hearts.

## IV. CONCLUSION

In this study, we developed and validated a novel  $E_{es}$  calculation approach based on machine learning technology for ESHP. Experimental results confirmed that the single-beat  $E_{es}$  calculation method correlated well with the conventional method over a wide range of cardiac contractility and loading conditions. Transplantation experimental results show that the  $E_{es}$  calculated using our method correlated well with the early post-transplant cardiac index. The proposed approach should be a useful tool to quantitatively assess left ventricular contractility during *ex situ* heart perfusion and estimate early post-transplant outcomes. To the best of our knowledge, the approach here described is the only study to date to calculate  $E_{es}$  by estimating  $V_0$  from steady-state beats in ESHP and use it to predict early post-transplantation outcomes (CI).

### ACKNOWLEDGMENT

This paper is supported by the Dr. Michael R Freeman Innovation Award and Connaught Innovation Award. We thank

Denise Rooney from Medtronic Canada for the support and valuable comments for our research.

## REFERENCES

- [1] B. A. e. a. Boilson, "Device therapy and cardiac transplantation for end-stage heart failure," *Current Problems in Cardiology*, vol. 35, no. 1, pp. 8–64, 2010.
- [2] A. C. e. a. Gaffey, "Transplantation of "high-risk" donor hearts: Implications for infection," *J Thorac Cardiovasc Surg*, vol. 152, no. 1, pp. 213–220, 2016.
- [3] E. M. Hsich, "Matching the market for heart transplantation," *Circ Heart Fail*, vol. 9, no. 4, p. e002679, 2016.
- [4] K. S. e. a. Dujardin, "Myocardial dysfunction associated with brain death: Clinical, echocardiographic, and pathologic features," *Journal of Heart & Lung Transplantation*, vol. 20, no. 3, pp. 350–357, 2001.
- [5] M. J. e. a. Collins, "Preserving and evaluating hearts with ex vivo machine perfusion: an avenue to improve early graft performance and expand the donor pool," *European Journal of Cardio-Thoracic Surgery*, vol. 34, no. 2, pp. 318–325, 2008. [Online]. Available: [Go to ISI://WOS:000258518400016](https://doi.org/10.1017/S1091-017-0882-5)
- [6] A. e. a. Ardehali, "Ex-vivo perfusion of donor hearts for human heart transplantation (proceed ii): a prospective, open-label, multicentre, randomised non-inferiority trial," *Lancet*, vol. 385, no. 9987, pp. 2577–2584, 2015.
- [7] J. e. a. Beuth, "New strategies to expand and optimize heart donor pool: Ex vivo heart perfusion and donation after circulatory death: A review of current research and future trends," *Anesthesia and Analgesia*, vol. 128, no. 3, pp. 406–413, 2019. [Online]. Available: [Go to ISI://WOS:000460108900015](https://doi.org/10.1017/S1091-017-0882-5)
- [8] A. e. a. Iyer, "Increasing the tolerance of dcd hearts to warm ischemia by pharmacological postconditioning," *American Journal of Transplantation*, vol. 14, no. 8, pp. 1744–1752, 2014.
- [9] P. e. a. Leprince, "Ex vivo perfusion of the heart with the use of the organ care system," *European journal of cardio-thoracic surgery : official journal of the European Association for Cardio-thoracic Surgery*, vol. 49, no. 5, p. 1318, 2016.
- [10] J. M. e. a. Trahanas, "Achieving 12 hour normothermic ex situ heart perfusion: An experience of 40 porcine hearts," *Asaio Journal*, vol. 62, no. 4, p. 470, 2016.
- [11] M. T. e. a. Sodums, "Evaluation of left ventricular contractile performance utilizing end-systolic pressure-volume relationships in conscious dogs," *Circulation Research*, vol. 54, no. 6, pp. 731–739, 1984.
- [12] R. G. e. a. McKay, "Assessment of the end-systolic pressure-volume relationship in human beings with the use of a timevarying elastance model," *Circulation*, vol. 74, no. 1, pp. 97–104, 1986.
- [13] H. C. e. a. Mehmel, "The linearity of the end-systolic pressure-volume relationship in man and its sensitivity for assessment of left ventricular function," *Circulation*, vol. 63, no. 6, pp. 1216–1222, 1981.
- [14] M. J. Barber, "Effect of time interval between repeated brief coronary artery occlusions on arrhythmia, electrical activity and myocardial blood flow," *Journal of the American College of Cardiology*, vol. 2, no. 4, pp. 699–705, 1983.
- [15] M. T. e. a. Vivaldi, "Triphenyltetrazolium staining of irreversible ischemic injury following coronary artery occlusion in rats," *American Journal of Pathology*, vol. 121, no. 3, p. 522, 1985.
- [16] T. e. a. Noto, "Temporal and topographic profiles of tissue hypoxia following transient focal cerebral ischemia in rats," *Journal of Veterinary Medical Science*, vol. 68, no. 8, p. 803, 2006.
- [17] F. L. Abel, "Pmax, end systolic elastance, and starling's law of the heart," *Shock*, vol. 15, no. 1, pp. 56–9, 2001.
- [18] S. e. a. K, "Estimation of the hydromotive source pressure from ejecting beats of the left ventricle," *IEEE transactions on bio-medical engineering*, vol. 27, no. 6, pp. 299–305, 1980.
- [19] M. e. a. Takeuchi, "Single-beat estimation of the slope of the end-systolic pressure-volume relation in the human left ventricle," *Circulation*, vol. 83, no. 1, pp. 202–12, 1991. [Online]. Available: <https://www.ncbi.nlm.nih.gov/pubmed/1898642>
- [20] E. A. e. a. Ten Brinke, "Single-beat estimation of the left ventricular end-systolic pressure-volume relationship in patients with heart failure," *Heart*, vol. 198, no. 1, pp. 37–46, 2010.
- [21] C. H. e. a. Chen, "Noninvasive single-beat determination of left ventricular end-systolic elastance in humans," *Journal of the American College of Cardiology*, vol. 38, no. 7, pp. 2028–2034, 2001. [Online]. Available: [Go to ISI://WOS:000172458000039](https://doi.org/10.1017/S1091-017-0882-5)
- [22] T. e. a. Shishido, "Single-beat estimation of end-systolic elastance using bilinearly approximated time-varying elastance curve," *Circulation*, vol. 102, no. 16, pp. 1983–1989, 2000. [Online]. Available: [Go to ISI://WOS:000089856000021](https://doi.org/10.1161/01.CIR.102.16.1983)
- [23] X. e. a. Lin, "A support vector machine-recursive feature elimination feature selection method based on artificial contrast variables and mutual information," *Journal of Chromatography B*, vol. 910, no. 23, pp. 149–155, 2012.
- [24] C. C. M. e. a. Davi, "Severe dengue prognosis using human genome data and machine learning," *IEEE Transactions on Biomedical Engineering*, pp. 1–1, 2019.
- [25] T. M. e. a. Caro, "Inter-observer reliability," *Behaviour*, vol. 69, no. 3/4, pp. 303–315, 1979.
- [26] M. Awad and R. Khanna, "Support vector regression," *Neural Information Processing Letters & Reviews*, vol. 11, no. 10, pp. 203–224, 2007.
- [27] K. e. a. Luu, "Age estimation using active appearance models and support vector machine regression," in *Biometrics: Theory, Applications, and Systems, 2009. BTAS '09. IEEE 3rd International Conference on*, 2009, Conference Proceedings.
- [28] R. M. Balabin and E. I. Lomakina, "Support vector machine regression (svr/lsvm) - an alternative to neural networks (ann) for analytical chemistry? comparison of nonlinear methods on near infrared (nir) spectroscopy data," *Analyst*, vol. 136, no. 8, p. 1703, 2011.
- [29] L. e. a. Xin, "A new multi-mode perfusion system for ex vivo heart perfusion study," *Journal of Medical Systems*, vol. 42, no. 2, p. 25, 2017. [Online]. Available: <https://doi.org/10.1007/s10916-017-0882-5>
- [30] J. B. e. a. Ryan, "Cariporide (hoe-642) improves cardiac allograft preservation in a porcine model of orthotopic heart transplantation," *Transplantation*, vol. 12, no. 2, pp. A29–A29, 2003.
- [31] K. Sagawa, "The end-systolic pressure-volume relation of the ventricle: definition, modifications and clinical use," *Circulation*, vol. 63, no. 6, pp. 1223–1227, 1981.
- [32] S. e. a. Davidson, "Minimally invasive estimation of ventricular dead space volume through use of frank-starling curves," *Plos One*, vol. 12, no. 4, 2017. [Online]. Available: [Go to ISI://WOS:000400383600057](https://doi.org/10.1371/journal.pone.0170057)
- [33] T. e. a. Nozawa, "Efficiency of energy transfer from pressure-volume area to external mechanical work increases with contractile state and decreases with afterload in the left ventricle of the anesthetized closed-chest dog," *Circulation*, vol. 77, no. 5, pp. 1116–24, 1988. [Online]. Available: <https://www.ncbi.nlm.nih.gov/pubmed/3359589>
- [34] J. E. Hall, *Guyton and Hall textbook of medical physiology*, 13th ed. Philadelphia, PA: Elsevier, 2016.
- [35] V. H. Cao and M. Ahmed, "Application of support vector regression trained by particle swarm optimization in warrant price prediction," *Monografias Inia Agrícola*, vol. 114, no. 47, pp. 1466–8, 2010.
- [36] Q. e. a. Meng, "Forecasting of coal seam gas content by using support vector regression based on particle swarm optimization," *Journal of Natural Gas Science & Engineering*, vol. 21, no. 21, pp. 71–78, 2014.
- [37] P. e. a. Niu, "Optimized support vector regression model by improved gravitational search algorithm for flatness pattern recognition," *Neural Computing & Applications*, vol. 26, no. 5, pp. 1167–1177, 2015.
- [38] A. Swami and R. Jain, "Scikit-learn: Machine learning in python," *Journal of Machine Learning Research*, vol. 12, no. 10, pp. 2825–2830, 2012.
- [39] D. V. Cicchetti, "Guidelines, criteria, and rules of thumb for evaluating normed and standardized assessment instruments in psychology," *Psychological Assessment*, vol. 6, no. 4, pp. 284–290, 1994.
- [40] J. Zar, "Significance testing of the spearman rank correlation coefficient," *Publications of the American Statistical Association*, vol. 67, no. 339, pp. 578–580, 1972.
- [41] A. e. a. Kono, "Use of left ventricular end-ejection pressure and peak pressure in the estimation of the end-systolic pressure-volume relationship," *Circulation*, vol. 70, no. 6, pp. 1057–65, 1984.
- [42] G. Blaudszun and D. R. Morel, "Relevance of the volume-axis intercept, v0, compared with the slope of end-systolic pressure-volume relationship in response to large variations in inotropy and afterload in rats," *Experimental Physiology*, vol. 96, no. 11, pp. 1179–1195, 2011. [Online]. Available: [\[Go to ISI://WOS:000297150800009\]](https://doi.org/10.1113/EXP060117)